

Response of Arabian Sea to the local forcing during 2003 pre-monsoon warming phase

J. S. CHOWDARY, C. GNANASEELAN*, BIJOY THOMPSON, S. K. SINHA

and

P. S. SALVEKAR

Indian Institute of Tropical Meteorology, Pune – 411008, India

*e mail : seelan@tropmet.res.in

सार—दक्षिणी पश्चिमी मानसून के आरंभ होने से पहले महासागर का सबसे उष्ण भाग (समुद्र सतह तापमान $> 30.5^\circ$ से.) अरब सागर के दक्षिणी पूर्वी भाग में ज्ञात किया गया है। अरब सागर मानसून प्रयोग (आरमेक्स), मार्च और अप्रैल 2003 के दौरान अरब सागर के दक्षिण पूर्व में उष्ण जलकुंड बनने और जून के महीने में उसके समाप्त होने से संबंधित प्रक्रियाओं को समझने का सुनहरा अवसर प्रदान करता है। इससे यह ज्ञात हुआ है कि आरमेक्स से समुद्र सतह तापमान के साप्ताहिक विश्लेषण और मार्च के ही अंतिम सप्ताह में उष्णकटिबंधीय वर्षा मापन मिशन (टी. आर. एम. एम.) सूक्ष्म तरंग बिम्बप्रेक्षण (टी. एम. आई.) में दक्षिणी पूर्वी अरब सागर पर समुद्र सतह तापमान 29.5° से. से अधिक हो जाता है। आरमेक्स और टी. एम. आई. आंकड़ों के साथ विक्कस्कैट सतह के निकट पवनों का उपयोग इस क्षेत्र में पवन से प्रवर्तित ट्रांसपोर्ट की भूमिका की जाँच के लिए किया गया है और इससे यह पता चला है कि अरब सागर की दक्षिणी परिसीमा (8° उ.) दक्षिणी पश्चिमी मानसून अवधि के दौरान दक्षिणाभिमुखी थी और शीतकालीन मानसून ऋतु की अवधि में उत्तराभिमुखी थी। मार्च और अप्रैल में कमजोर ट्रांसपोर्ट और दक्षिणी पूर्वी अरब सागर पर सूर्य के ताप में वृद्धि उष्ण जलकुंड के संवर्धन की अवस्था में सहायक होती है। मई 2003 के अंतिम सप्ताह से एकमन सतह के निचले भाग पर उर्ध्वाधर वेग धीरे-धीरे बढ़ता हुआ मानसून के आरंभ के बाद उच्चतर मान प्राप्त कर लेता है जो शीतल जल और सतह को ठंडा करने में सहायक होते हैं। यह शीतलन सोमाली तट से शीतल जल के अपतटीय अभिवहन द्वारा और उत्तरी अरब सागर से उच्च लवणता ट्रांसपोर्ट के कारण भी होता है।

ABSTRACT. Prior to the onset of south west monsoon the warmest part of the ocean ($SST > 30.5^\circ C$) has been observed in the South Eastern Arabian Sea (SEAS). Arabian Sea Monsoon Experiment (ARMEX) provided an excellent opportunity to understand the processes that are associated with the formation of warm pool over SEAS during March and April 2003 and its collapse in June. It is observed that SST over SEAS exceeds $29.5^\circ C$, in the weekly SST analysis from ARMEX and Tropical Rainfall Measuring Mission (TRMM) Micro wave Imager (TMI) observations in the last week of March itself. Along with ARMEX and TMI data, Quikscat near surface winds have been used in the study to examine the role of wind driven transport in this region and it was found that at southern boundary ($8^\circ N$) of the Arabian Sea the transport was southward during southwest monsoon period and northward in the winter monsoon period. In March and April the weak transports and the increase in the insolation over the SEAS are supporting the growing phase of warm pool. The vertical velocity at the bottom of Ekman layer gradually increasing from last week of May 2003 and attains higher value after onset of monsoon, which helps to bring up the cold water and cool the surface. The cooling also is caused by the offshore advection of cold water from Somali coast and high salinity transport from northern Arabian Sea.

Key words – ARMEX, Arabian Sea, Warm pool, Ekman transport, Sverdrup transport.

1. Introduction

The zones of atmospheric convective movements always remain over the warmest surface water of the ocean. The largest region of warm water lies in the western Pacific and Eastern Indian Ocean (EIO), this

warm pool is the product of interaction between the ocean and atmosphere (Webster and Lukas 1992). Krishnamurti *et al.* (1988) showed that the region of pronounced intraseasonal variance in SST lies over the tropical western Pacific and EIO. This Indo-Pacific warm pool influences the strength and location of atmospheric

convection and hence governing the large scale circulation. Across the entire warm pool the net surface heat flux leads the SST variation and the surface heat flux variations are driving the SST variations at these intraseasonal timescales (Shinoda *et al.*, 1998).

A warm pool during pre-monsoon season in the Arabian Sea with a tongue of highly warm water surface mass ($>30.8^{\circ}\text{C}$) was first reported by Seetaramayya and Master (1984), between the 8°N to 15°N and 65°E to 75°E . This warm pool is recognized as a mini-warm pool of the Indian Ocean (Rao and Sivakumar 1999). They described that in the Arabian Sea the surface water progressively warms up during the pre-monsoon season, attaining high SST in the south east region just before the onset of summer monsoon. This abnormal behaviour of Arabian Sea is due to the influence of seasonally reversing monsoonal winds during southwest and northeast monsoon periods. The direct effect of increasing the SST is to increase the transfer of heat and moisture from ocean into the atmosphere (Kershaw, 1985). Shetye (1986) concluded that it is not possible to simulate the Arabian Sea SST realistically during the southwest monsoon unless both thermodynamics and dynamics are adequately modeled. Since the warm pool of SEAS collapse immediately after the onset of southwest monsoon, it is necessary to investigate both dynamics and thermodynamics responsible for the damping phase of warm pool. Rao and Sivakumar (1999) also observed that south east Arabian Sea is dynamically and thermodynamically active during pre monsoon and summer monsoon seasons.

This warm water enhances the sensitivity of monsoonal atmosphere to small thermal changes in the upper ocean in view of non linear relationship between SST and evaporation (Rao and Sivakumar 1999). The processes that are influencing the mini warm pool are of particular interest since it may have an effect on the onset of monsoon and the development of storms over that region. It is important to know the existence of Arabian Sea mini warm pool, the mechanism responsible for evolution and dissipation of warm pool with sophisticated model and observational studies. In order to fulfill this, the ARMEX Phase-II marine observational program was carried out during 2003 pre-monsoon and monsoon periods. The time series observations were collected, the first during 22 March to 7 April, which is the growing phase of the warm pool and the second during 22 May to 7 June 2003, the mature phase of warm pool in the SEAS. In this study we have used ARMEX SST observations during 22 March - 7 April and TMI SST for the pre-monsoon and monsoon periods, to examine the evolution and collapse of SEAS warm pool during 2003 ARMEX

observational period. The role of wind driven transport is also studied using Quikscat surface winds during the same period.

2. Materials and methods

In the present study we have used SST data collected during ARMEX cruise from 22 March – 7 April. Based on Barnes (1964) objective analysis scheme, the observed SSTs are objectively analysed over the SEAS. The Barnes objective map analysis scheme is computationally simple in which Gaussian weight to a datum is a function of distance between datum and grid points. The weight W is assumed according to the distance R between the datum and grid point as,

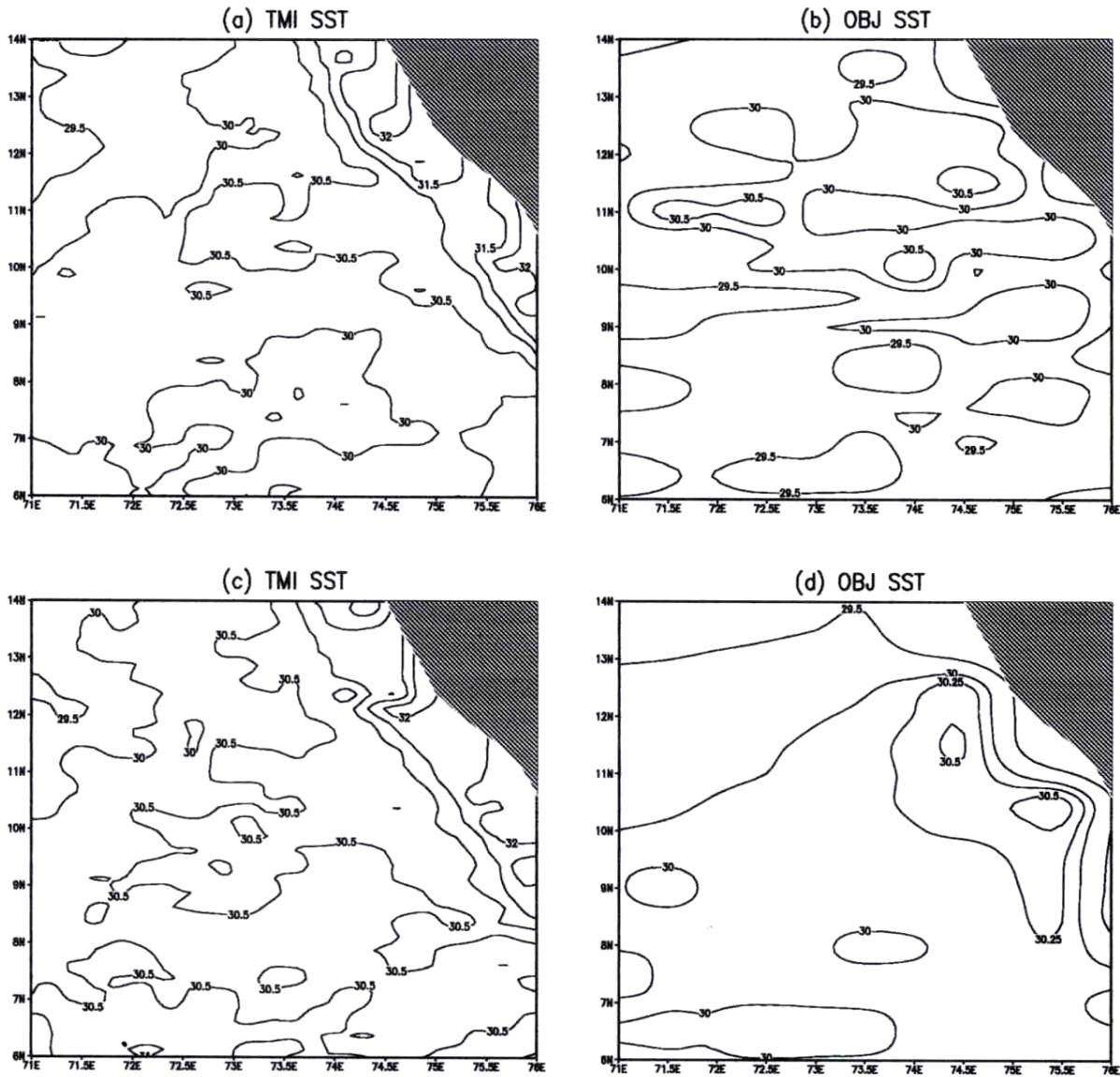
$$W = \exp(-R^2/k) \quad (1)$$

Where $k = 5.052 (2 \Delta n / \pi)^2$ is length scale.

The domain of our analysis is bounded by 71°E to 76°E and 6°N to 14°N (here after study region) with grid resolution of 0.5° . Petersen and Middleton (1963) stated that a wave whose horizontal wave length does not exceed at least $2\Delta n$ (Δn is the average data spacing) cannot be resolved since five data points are required to describe a wave. Hence Δx (grid resolution) should not be larger than $\Delta n/2$. Since very small resolution may produce an unrealistic noise derivative and if derivative fields have to represent only resolve features, the grid length should not be much smaller than Δn . Thus a constraint that $\Delta n/3 \leq \Delta x \leq \Delta n/2$ was imposed by Barnes in his interactive scheme.

The objectively analyzed SST (OBJ SST) field has been compared with TMI SST fields of resolution $0.25^{\circ} \times 0.25^{\circ}$ within the study region. The daily TMI SST data have been averaged to weekly data for the period March to June, 2003.

Near surface wind speed and directions are routinely observed by ships and buoys, inferred from satellite scatterometer measurements, and simulated from the atmospheric general circulation models. Ship wind observations are too sparse to delineate the Somali jet over Arabian Sea. Wind direction over Arabian Sea is south westerly during June to September (*i.e.*, south west monsoon) and north easterly during December to March (*i.e.*, north east monsoon). July wind stress in Arabian Sea is 2 -3 times larger than that in January. The sea winds scatterometer on Quikscat satellite is a microwave radar launched and operated by the US National Aeronautics and Space Administration (NASA). From 25 km measurements across a 1600 km swath, Quikscat winds samples more than 90% of global ocean every 24 hour.



Figs. 1(a-d). Weekly average SST (°C) in 2003 (a&b) 25 to 31 March and (c&d) 1 to 7 April

Wind stress over the Arabian Sea was computed with Quikscat wind velocity vector using the bulk aerodynamic formula:

$$\tau_x = \rho_o C_d u \cdot U \quad (2)$$

$$\tau_y = \rho_o C_d v \cdot U \quad (3)$$

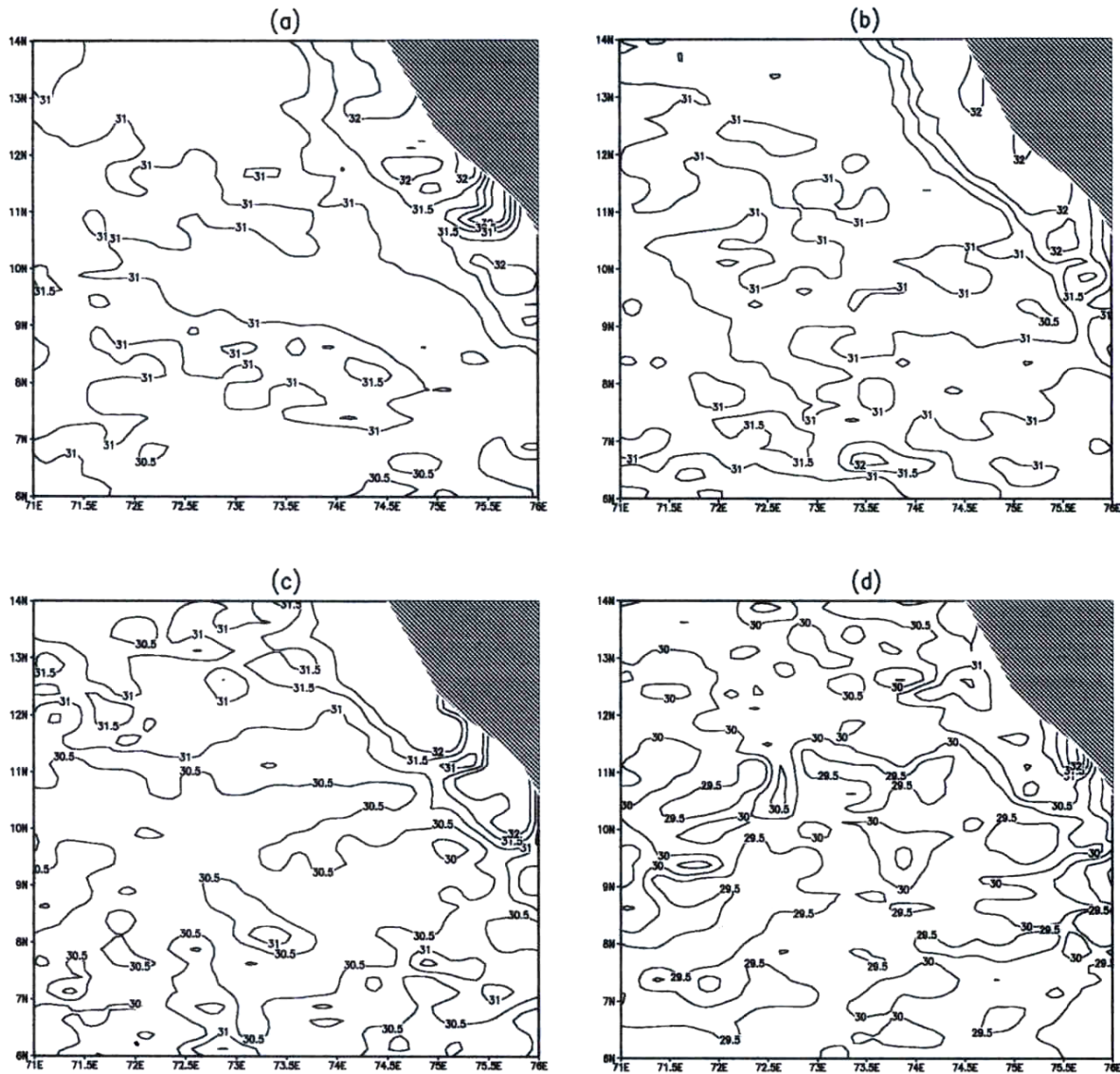
Where U is the wind speed, which is equal to $(u^2+v^2)^{1/2}$, ρ_o is air density (1.25 kg/m^3) and C_d is non dimensional drag coefficient (1.10×10^{-3}). Wind driven transports such as vertical transport at the bottom of

Ekman layer, meridional Ekman transport and Sverdrup transports are computed with Quikscat wind stress according to Stommel (1965) which are given below.

The vertical velocity at the bottom of the Ekman layer :

$$W_E = (1 / \rho f) (\text{curl}_z \tau + \beta \tau_x / f) \quad (4)$$

Here the Coriolis parameter f is equal to $2\Omega \sin \varphi$, where φ is the latitude, Ω is the rotation rate of Earth ($7.29 \times 10^{-5} \text{ rad s}^{-1}$), and β , the rate of change of the Coriolis parameter with latitude, is equal to $2\Omega \cos \varphi / R$,



Figs. 2(a-d). Weekly average of TMI SST ($^{\circ}\text{C}$) IN 2003 (a) 25 to 31 May (b) 1 to 7 June (c) 8 to 14 June and (d) 15 to 21 June

with R equal to the radius of Earth (6.37×10^6 m). $\text{curl}_z \tau$, the vertical component of wind stress curl, is defined by,

$$\text{curl}_z \tau = \partial \tau_y / \partial x - \partial \tau_x / \partial y \quad (5)$$

The meridional Ekman transport per unit zonal width is computed as,

$$-\tau_x / \rho f \quad (6)$$

Sverdrup transport per unit zonal width is,

$$\text{curl}_z \tau / \rho \beta \quad (7)$$

3. Results and discussion

During the pre-monsoon season, under clear skies and light wind conditions the radiative heat input overwhelms turbulent heat exchange at the air-sea interface and net surplus energy is absorbed in a shallow and weakly stratified near surface layer resulting in the formation of mini warm pool over SEAS (Rao and Sivakumar 1999). The SST of mini warm pool in the Arabian Sea has been recognised as an important boundary condition, which may trigger the onset of the southwest monsoon and may promote the formation of the onset vortex. The SST high starts forming in February and in March – April the mini warm pool formation begins

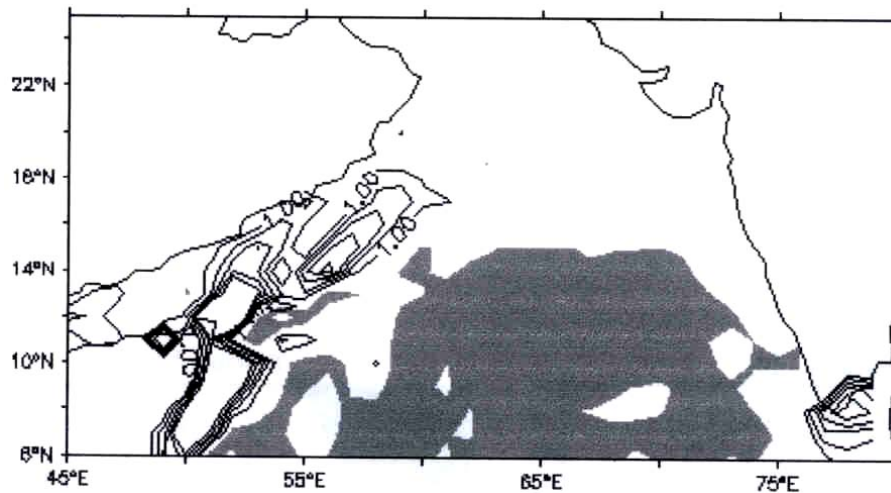


Fig. 3. Vertical velocity at bottom of Ekman layer for July 2003 (contour interval is $10 \times 10^{-6} \text{ m s}^{-1}$ and negative values are shaded)

(growing phase) with SST higher than 29.5° C . In the present paper OBJ SST from ARMEX observation for the period (25 March - 7 April, 2003) was compared with TMI SST. Even though the ARMEX data is available for the period of 22 March to 7 April, we divided the data into two parts (weekly) and performed the objective analysis in order to observe how warm pool in the study region was progressing during growing phase of 2003. In the last week of March (weekly averaged SST) both the TMI SST [Fig. 1(a)] and the OBJ SST [Fig. 1(b)] show SST greater than 29.5° C over the study region. In both TMI and OBJ SST most of the region was warmer than 30° C and in some part of the region SST was above 30.5° C . It shows that the SST over this region is much larger than the threshold value (28° C), which is a necessary condition for the deep convection in tropics. However the SST greater than 28° C is not sufficient for deep convection because of light winds, insufficient moisture availability due to dry wind and large scale subsidence are not promoting the convective activity in March and April. Figs. 1(c&d) show the TMI and OBJ SST for the period April 1-7 (weekly mean) respectively. It is observed that TMI SST shows slightly higher values than OBJ SST. It is interesting to note that the increase of TMI SST is observed in April first week over the Arabian Sea compared to the last week of March, the same can be seen in the OBJ SST as almost entire area south of 11° N was warmer than 30° C . A considerable increase in weekly SST was observed in both TMI and OBJ SST during the growing stage of mini warm pool.

The warm pool reaches its matured phase, *i.e.*, SSTs greater than 30.5° C prior to the onset of summer monsoon. The year 2003 was a normal monsoon year but

was characterized by late onset over Kerala (8 June) and rainfall covered entire country on 5th July, 10 days prior to normal date. Here we examined the TMI SST in the mature and decay phase of warm pool before and after the onset of monsoon in 2003. Daily TMI SST averaged for weekly for the period of 25 - 31 May, 1 - 7 June (before the onset of monsoon), 8 - 14 June and 15 - 21 June (after onset of monsoon) are shown in Fig. 2. Most of the region in the study area was covered with 31° C contours both in May last week [Fig. 2(a)] and June first week [Fig. 2(b)]. The SSTs are slightly more in southern part of study area in the first week of June. However maximum SST over SEAS was observed one week prior to the onset of monsoon 2003. SST high would occur in all seasons in April and May. So the observed delay in 2003 monsoon onset was clearly due to the atmospheric processes (instabilities) in spite of the presence of high SST. Soon after the onset of monsoon on June 8, the winds strengthened and SST decreased by 0.5° C over most of the study region [Fig. 2(c)], in the third week of June 2003 the SSTs are further reduced by 0.5 to 1° C . After the appearance of Somali Jet the SST decreases initially in the western Arabian Sea due to upwelling of cold water from below. With the onset of monsoon, Arabian Sea winds progress towards India, the SEAS warm pool collapses due to the entrainment cooling from below and offshore advection of cold water from coastal upwelling areas (off the Somali coast).

3.1. Wind driven ocean transports

A thick barrier layer forms in SEAS during northern winter due to arrival of low salinity water from Bay of Bengal (Shenoi *et al.*, 1999). The barrier layer survives till

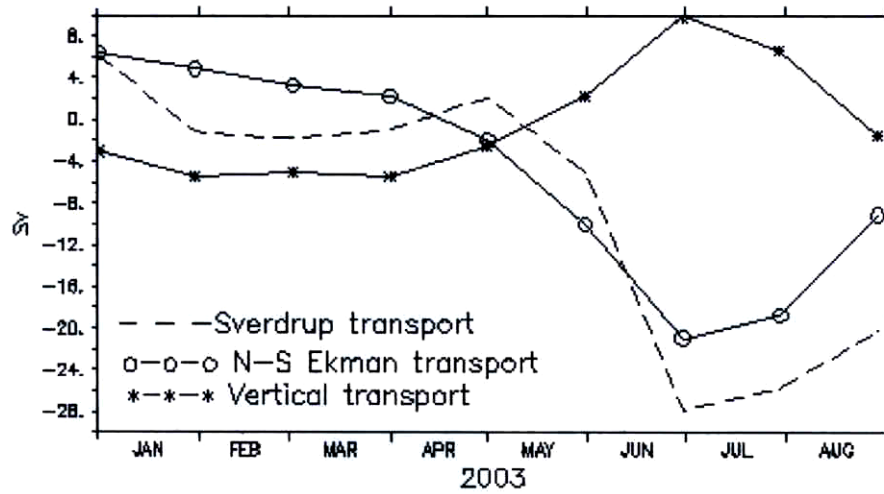


Fig. 4. Monthly mean vertical transports into the Ekman layer of Arabian Sea north of 8° N, meridional Ekman transports along 8° N and Sverdrup transports along 8°N in 2003

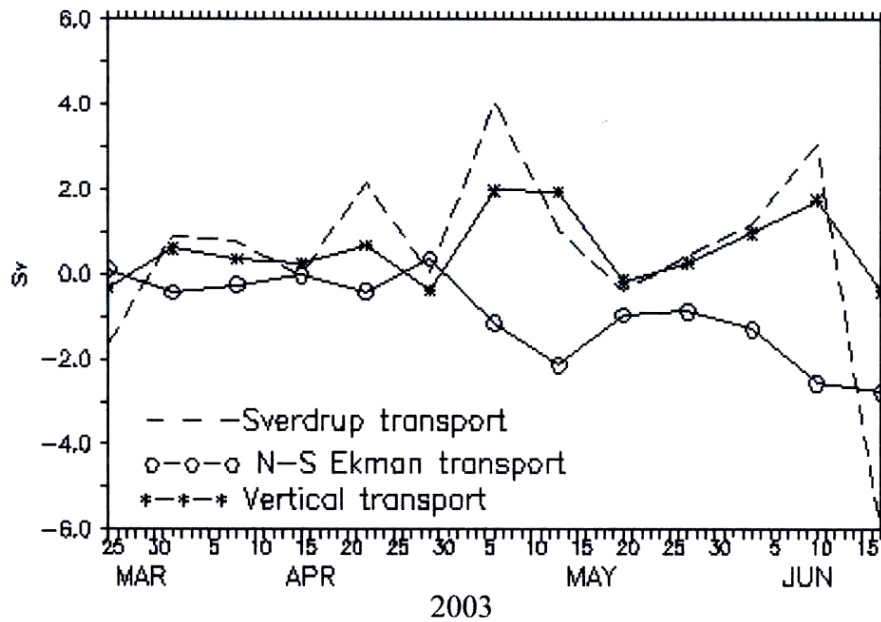
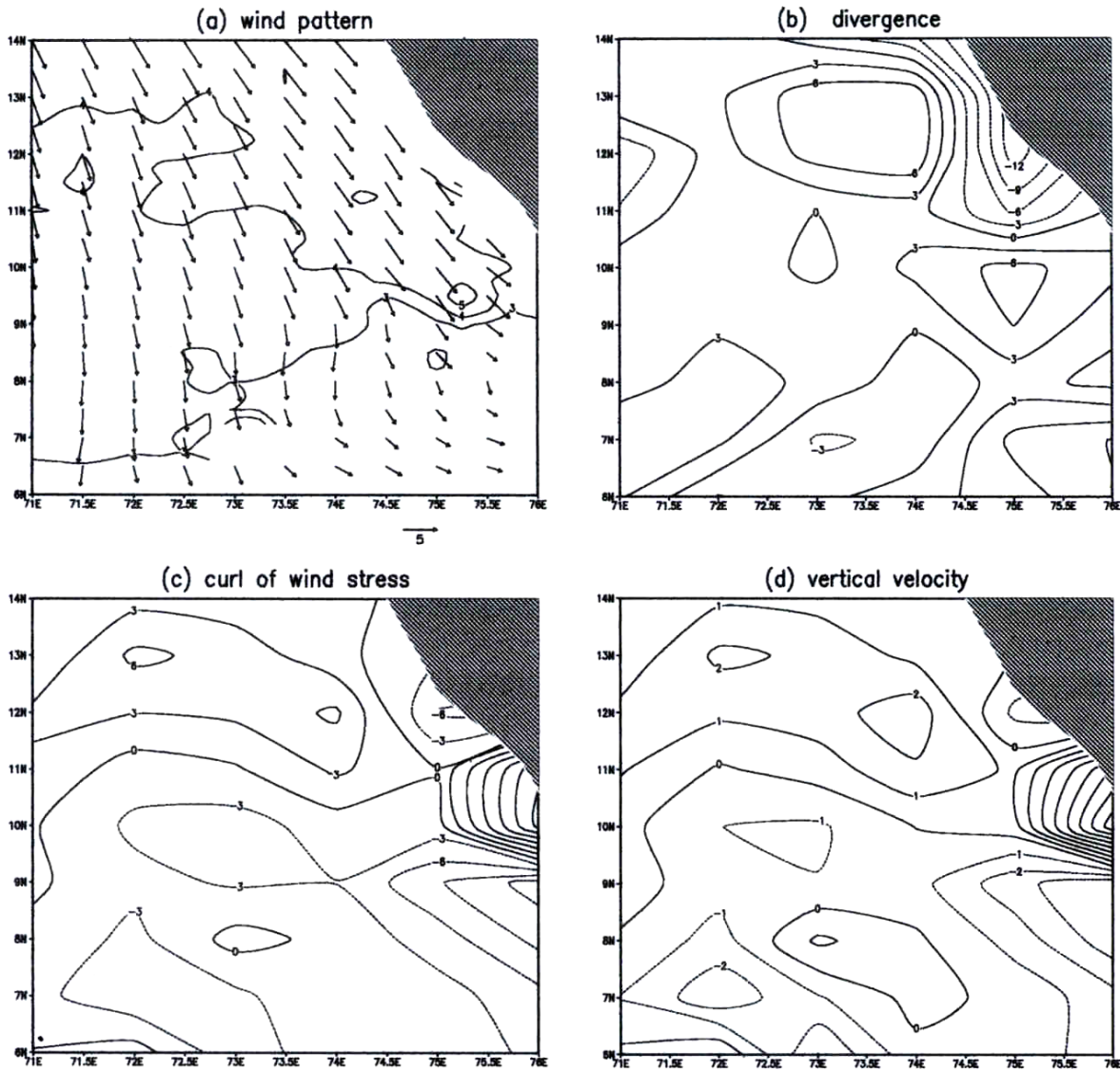


Fig. 5. Weekly averaged vertical transports into the Ekman layer of Arabian Sea between 7° N & 14° N and 71° E & 75° E and meridional Ekman transports and Sverdrup transport along 8° N, Zonally integrated between 71° E & 75° E in 2003 during pre monsoon season

end of May and is annihilated by the inflow of high salinity water from the north. This barrier layer traps momentum flux within the surface layer and avoid the entrainment cooling of mixed layer. However earlier studies revealed that ocean dynamics play a major role in

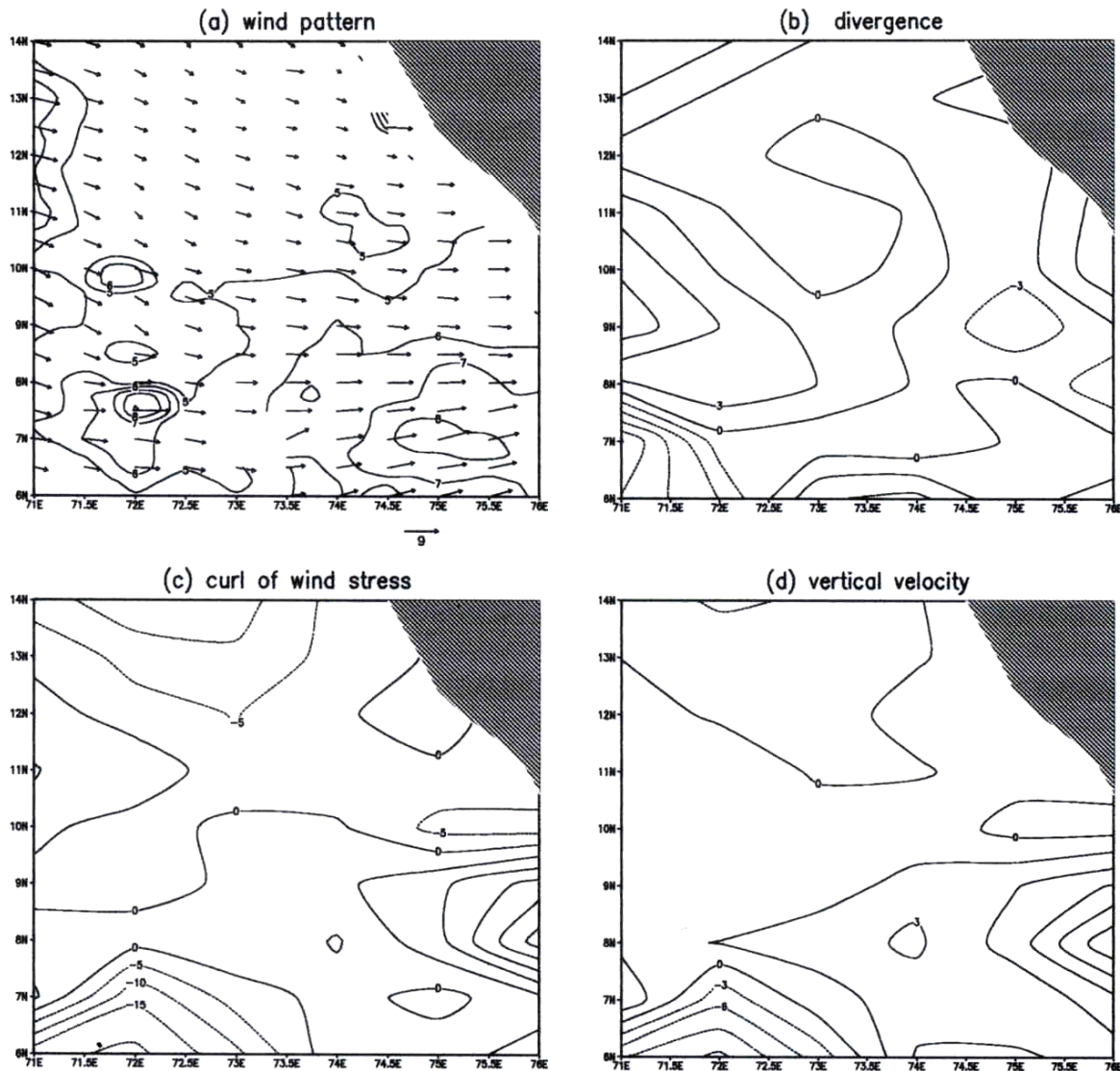
the formation, maintenance and collapse of the SST high in SEAS. Nevertheless winds over Arabian Sea are weak during March to May, non negligible wind driven transport are observed. The wind driven transport also contributes for movement of water mass along with



Figs. 6(a-d). Weekly average (a) Wind pattern (b) Divergence of wind field (contour interval is $1 \times 10^{-6} \text{ s}^{-1}$) (c) Curl of the wind stress field (contour interval is $1 \times 10^{-8} \text{ N m}^{-3}$) and (d) Vertical velocity at bottom of Ekman layer (contour interval is $1 \times 10^{-6} \text{ m s}^{-1}$), during 25-31 March 2003

oceanic currents towards the SEAS from Bay of Bengal in winter season and from north Arabian Sea in southwest monsoon season. Vertical velocities for the month of July (monthly mean, Fig. 3) in the Arabian Sea are compared with results produced by Halpern *et al.* (1998). It is observed that the vertical velocities computed from Quikscat wind fields are very well matching with the water raising (very weak upward motion except in the Oman and Somali region) in the north of 11° N and sinking (downward motion), which is shaded in the figure, south of 11° N in the Arabian Sea.

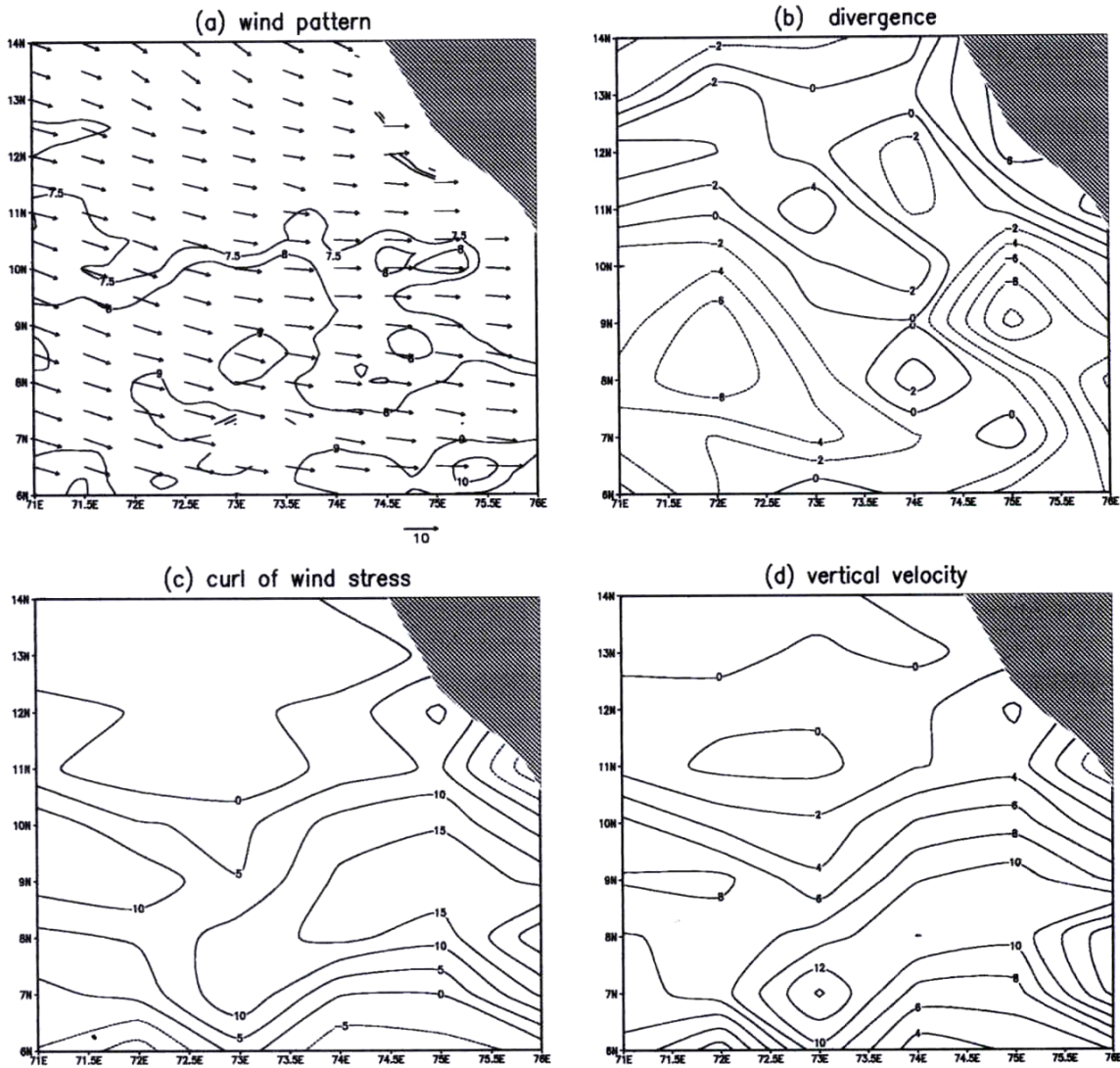
Mean monthly vertical transport at the bottom of Ekman layer over the Arabian Sea (north of 8° N), meridional Ekman transport and Sverdrup transport along the Arabian Sea at 8° N were computed using Quikscat surface wind fields. Fig. 4 shows time series of the zonally integrated values of north south Ekman transport and Sverdrup transport between 52° E and 75° E correspond to the Arabian Sea at 8° N during 2003. Halpern *et al.*, (1998) computed the meridional Ekman transport and Sverdrup transport along the southern boundary of Arabian Sea at 8.5° N from IFR2 wind



Figs. 7(a-d). Weekly average (a) Wind pattern (b) Divergence of wind field (contour interval is $1 \times 10^{-6} \text{ s}^{-1}$) (c) Curl of the wind stress field (contour interval is $1 \times 10^{-8} \text{ N m}^{-3}$) and (d) Vertical velocity at bottom of Ekman layer (contour interval is $1 \times 10^{-6} \text{ m s}^{-1}$), during 25-31 May 2003

velocity data created from radar backscattered, measured by the first European Remote Sensing Satellite (ERS-1) data, during the period May 1992 – May 1996 and suggested that month to month variations of wind driven transport was similar for each year. The wind driven transports of 2003 are very well comparable with the results of Halpern *et al.*, (1998), however there was a little difference in magnitude, which may be due to interannual variability. The maximum negative (southward) Ekman transport and Sverdrup transport occurred in July and also positive (northward) Ekman transport occurred during northeast monsoon period with the maximum in the month of November and attain negative value from the month of April. The vertical transport over the Arabian

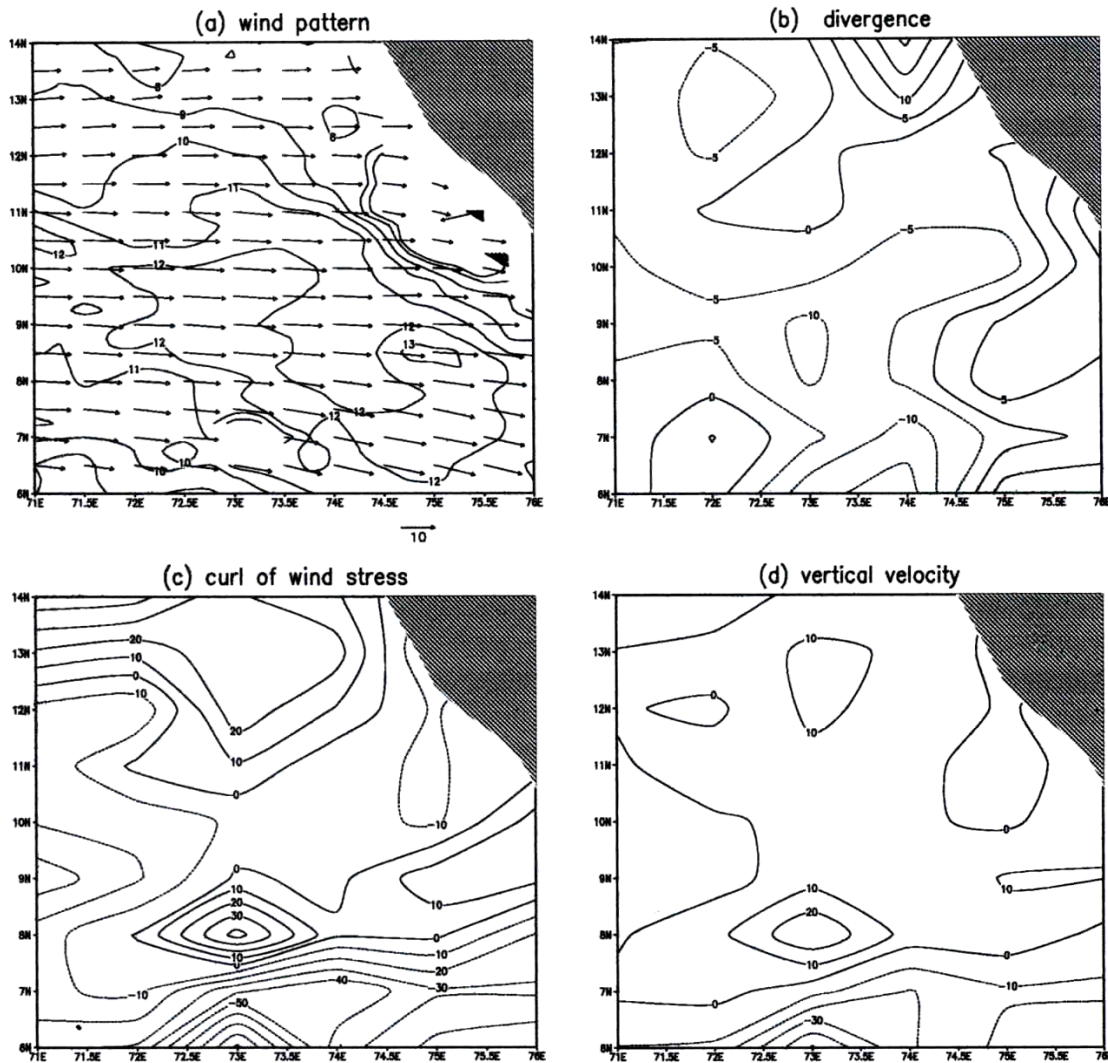
Sea north of 8° N is shown in Fig. 4 where maximum positive value observed in the beginning of July and gradually decreases thereon. The time series of zonal transport in upper 300 meter is calculated by Schott *et al.* (1994) from mooring for latitude range $3^\circ 45' \text{ N} - 5^\circ 52' \text{ N}$, south of Sri Lanka during January 1991 – February 1992. They observed westward transport for the winter monsoon, also by using primitive equation model of the Geophysical Fluid Dynamics Laboratory for the Indian Ocean they confirmed that strong westward transport exists in winter monsoon with the amplitude of 11 Sv. Their study further supports the results obtained from Quikscat winds (northward transport in winter monsoon at 8° N).



Figs. 8(a-d). Weekly average (a) Wind pattern (b) Divergence of wind field (contour interval is $1 \times 10^{-6} \text{ s}^{-1}$) (c) Curl of the wind stress field (contour interval is $1 \times 10^{-8} \text{ N m}^{-3}$) and (d) Vertical velocity at bottom of Ekman layer (contour interval is $1 \times 10^{-6} \text{ m s}^{-1}$), during 1-7 June 2003

During the pre-monsoon season weekly mean vertical transport (across the bottom of the Ekman layer of the Arabian Sea north of 7° N to south of 14° N and east of 70° E), meridional Ekman transport and Sverdrup transport (along 8° N) are computed and plotted (Fig. 5) from 25 March – 15 June, 2003. Both north- south Ekman transport and Sverdrup transport are zonally integrated between 71° E and 75° E , which corresponds to SEAS. In the pre monsoon season Sverdrup transport shows more fluctuations than north south Ekman transport along 8° N over the study region. The maximum positive transport observed was 4 Sv in the first week of May and maximum negative value approximately -6 Sv seen after the onset of monsoon. Whereas meridional Ekman transport shows

gradually increasing trend towards negative value (southward transport) from 25 March – 15 June. Meridional transport was weak in March and April and from May onwards transport starts increasing negatively to a maximum value approximately -2 Sv after onset of monsoon. These transports may move high salinity water to southward over SEAS in the month of May and reaches its maximum after onset of monsoon, resulting in deepening of mixed layer over the study region and collapsing the barrier layer (Shenoi *et al.*, 1999). The vertical transport into the Ekman layer over the study region also shows small fluctuations. During March – April there was no considerable contribution of vertical transport as seen in the meridional Ekman transport, the



Figs. 9(a-d). Weekly average (a) Wind pattern (b) Divergence of wind field (contour interval is $1 \times 10^{-6} \text{ s}^{-1}$) (c) Curl of the wind stress field (contour interval is $1 \times 10^{-8} \text{ N m}^{-2}$) and (d) Vertical velocity at bottom of Ekman layer (contour interval is $1 \times 10^{-6} \text{ m s}^{-1}$), during 8-14 June 2003

magnitudes are high in May and June just before the onset of monsoon. However after the onset of monsoon the vertical transport increases resulting in cooling of SST over the SEAS [Fig. 2(a)]. It is important to note that the wind driven transport has a significant contribution towards the formation of warm pool over SEAS the positive (northward) transport from January - March [Fig. 2(a)] which helps to bring the low salinity water from Bay of Bengal. Also it contributes for collapsing the warm pool by increasing the southward transport after onset of monsoon which brings high saline water from the north Arabian Sea to SEAS.

The Quikscat wind direction and magnitudes are plotted in Fig. 6(a). The daily Quikscat surface wind data has been used for computing the horizontal divergence

(convergence), wind stress curl and vertical velocity at the bottom of Ekman layer over the study region as shown in [Figs. 6(b, c&d)] respectively. It is observed that during March first week wind speed was not exceeding 5m/s. The horizontal divergence of wind field shows that divergence component (positive) was dominant and there was no sign of convergence. Both wind stress curl and vertical velocities are positive (weak) north of 10° N and negative south of 10° N and this indicates that positive vertical velocity is responsible for upward motion and negative values for downward motion. There are two factors that can influence the surface layer and SST over this region, (i) the weak entrainment may not bring up the cold water due to the presence of barrier layer and light wind conditions, (ii) during December to April, the positive surface wind stress curl and associated Ekman divergence

shallows the pycnocline as pointed out by Rao and Sivakumar (1999). Almost similar features are found in the first week of April (not shown), only difference was that the magnitudes were slightly higher than last week of March.

Significant convergence before the onset of monsoon (*i.e.*, May last week and June first week during 2003), showed [Fig. 7(b) & Fig. 8(b)] over the study region mainly south of 10° N. In the last week of May, (*i.e.*, two weeks before the actual onset of monsoon) maximum wind speed observed was 8m/s [Fig. 7(a)]. The horizontal divergence is almost zero in the entire study region [Fig. 7(b)], which may be a sign for appearance of convergence in the upcoming weeks. Wind stress curl and vertical velocities [Figs. 7(c&d)] are also found weak in the last week of May. Wind speed reaches more than 9m/s just one week before the onset of monsoon [Fig. 8(a)] and the negative divergence (convergence) of wind field was appeared most of the study domain, which helps to enhance the convection and gives way for the onset of monsoon. Both wind stress curl and vertical velocity showed [Figs. 8 (c&d)] positive values which strengthen the entrainment over the SEAS. After the onset of monsoon the wind speed reaches more than 12m/s [Fig. 9(a)] and the convergence over the SEAS increases [Fig. 9(b)]. Negative wind stress curl south of 8.5° N and increases in vertical velocities after the onset of monsoon were observed [Figs. 9(c&d)]. The upward motion north of 7° N over the study region may be large enough to eliminate the barrier layer and brings up the cold water resulting in decrease in SST. Further in July offshore advected cold water from Somali coast cools the SST over the SEAS region.

4. Conclusion

ARMEX helped to provide data sets to understand the coupled ocean atmosphere and land processes and the thermodynamic processes occurring in Arabian Sea in the pre and post monsoon periods. The authors attempted a thorough study of the mechanism and structure of Arabian Sea warm pool during pre-monsoon phase of 2003. The objectively analyzed SST and TMI SST showed good agreement with each other. In the last week of March both the TMI and OBJ SSTs showed values greater than 29.5° C over the study region. TMI SST in the first week of April (mean of 1-7 April) showed slightly higher values (30.5° C) than that of OBJ SST (30° C). The week to week progress of warming was found to be very high especially in the warm pool growing phase.

The TMI SST showed that over the SEAS warm pool region temperatures crosses 31° C one week prior to

the onset of monsoon. The onset of monsoon was followed by decrease in SST in the SEAS, which was due to the appearance of Somali jet over SEAS. The offshore advection of cold water from Somali coast and entrainment of cold water force the cooling in SEAS. The meridional Ekman transport and Sverdrup transport were calculated (zonally integrated between 53° E and 75° E at 8° N) using Quikscat surface winds. The maximum southward Ekman transport and Sverdrup transport occurred in July and northward transport during northeast monsoon period. The vertical velocities (computed from Quikscat surface winds) during July 2003 showed upward motion present north of 11° N and sinking motion south of 11° N in the Arabian Sea. Also the vertical transport (computed) north of 8° N over the Arabian Sea was consistent with earlier studies. The Ekman and Sverdrup transports are zonally integrated between 71° E & 75° E along 8° N during pre monsoon in order to understand the role of wind driven transport over SEAS. The transports were weak in March and April 2003. Southward transport showed gradual increase after onset of monsoon. Large fluctuations in the Sverdrup transport were observed during the pre monsoon season. The vertical transport integrated 7° N – 14° N and 71° E – 75° E also showed some fluctuations with maximum value after onset of monsoon. Spatial and temporal structure of Quikscat wind divergence and vertical velocities over the SEAS found to have significant variations with convergence just before onset of monsoon, which is favourable for convective activities. The study highlights the importance of Quikscat winds in understanding the oceanic processes leading to SEAS SST high and its collapse. Also it is found that the wind driven transport has significant contribution towards the formation and collapse of warm pool.

Acknowledgements

The authors wish to acknowledge Department of Science and Technology, Government of India for conducting the ARMEX experiment and Department of Ocean Development, Government of India, for providing the financial support to carry out the work. We thank Frank Wentz, CA, USA for TMI data and for Quikscat data. Acknowledgements are also due to Director IITM, for his support. We also acknowledge P. Seetaramayya for scientific discussions. One of the co-author Bijoy Thompson acknowledges CSIR for financial support. The referee's valuable comments have helped us to improve the work.

References

- Barnes, S. L., 1964, "A technique for maximizing details in numerical weather map analysis", *J. Appl. Meteor.*, **3**, 396-406.

- Halpern, D. Freilich, M. H. and Weller, R. A., 1998, "Arabian Sea surface winds and ocean transports determined from ERS-1 scatterometer", *J. Geophys. Res.*, **103**, 7799-7805.
- Kershaw, R., 1985, "Onset of the southwest monsoon and SST anomaly in the Arabian Sea", *Nature*, **315**, 561-563.
- Krishnamurti, T. N., Oosterhof, D. K. and Mehta, A. V., 1988, "Air-sea interaction on the time scale of 30-50 days", *J. Atmos. Sci.*, **45**, 1304-1322.
- Peterson, D. P. and Middleton, D., 1963, "On representative observations", *Tellus*, **15**, 387-405.
- Rao, R. R. and Sivakumar, R., 1999, "On the possible mechanisms of the evolution of a mini-warm pool during the pre-summer monsoon season and the genesis of onset vortex in the south-eastern Arabian Sea", *Quart. J. Roy. Met. Soc.*, **125**, 787-809.
- Schott, F. Reppin, J. Fischer, J. and Quadfasel, D., 1994, "Current and transports of the Monsoon Current south of Sri Lanka", *J. Geophys. Res.*, **99**, 25, 127-25, 141.
- Seetharamayya, P. and Master, A., 1984, "Observed air-sea interface conditions and a monsoon depression during MONEX-79", *Arch. Met. Geoph. Biokl.*, **A33**, 61-67.
- Shenoi, S. S. C., Shankar, D. and Shetye, S. R., 1999, "On the sea surface temperature high in the Lakshadweep Sea before the onset of south west monsoon", *J. Geophys. Res.*, **104**, 15,703-15,712.
- Shetye, S. R., 1986, "A Model study of the seasonal cycle of the Arabian Sea surface temperature", *J. Mar. Res.*, **44**, 521-542.
- Shinoda, T., Hendon, H. H. and Glick, J., 1998, "Intraseasonal variability in the surface fluxes and sea surface temperature in the tropical western Pacific and Indian Ocean", *J. Climate*, **11**, 1685-1702.
- Stommel, H. M., 1965, "The Gulf Stream", Univ. of Calif. Press, Berkeley, p248.
- Webster, P. J. and Lukas, R., 1992, "TOGA/COARE: The coupled ocean-atmosphere response experiment", *Bull. Am. Meteorol. Soc.*, **73**, 1377-1416.
-